





ORIGINAL RESEARCH

Monocyte-Derived Macrophages Aggravate Cardiac Dysfunction After Ischemic Stroke in Mice

Hong-Bin Lin , MD, PhD; Pu Hong , MD; Meng-Yu Yin , MD; Zhi-Jun Yao, MD; Jin-Yu Zhang , MD, PhD; Yan-Pin Jiang, MD; Xuan-Xuan Huang, MD; Shi-Yuan Xu , MD; Feng-Xian Li , MD, PhD; Hong-Fei Zhang , MD, PhD

BACKGROUND: Cardiac damage induced by ischemic stroke, such as arrhythmia, cardiac dysfunction, and even cardiac arrest, is referred to as cerebral-cardiac syndrome (CCS). Cardiac macrophages are reported to be closely associated with stroke-induced cardiac damage. However, the role of macrophage subsets in CCS is still unclear due to their heterogeneity. Sympathetic nerves play a significant role in regulating macrophages in cardiovascular disease. However, the role of macrophage subsets and sympathetic nerves in CCS is still unclear.

METHODS AND RESULTS: In this study, a middle cerebral artery occlusion mouse model was used to simulate ischemic stroke. ECG and echocardiography were used to assess cardiac function. We used *Cx3cr1^{GFP}Ccr2^{RFP}* mice and *NLRP3*-deficient mice in combination with Smart-seq2 RNA sequencing to confirm the role of macrophage subsets in CCS. We demonstrated that ischemic stroke-induced cardiac damage is characterized by severe cardiac dysfunction and robust infiltration of monocyte-derived macrophages into the heart. Subsequently, we identified that cardiac monocyte-derived macrophages displayed a proinflammatory profile. We also observed that cardiac dysfunction was rescued in ischemic stroke mice by blocking macrophage infiltration using a *CCR2* antagonist and *NLRP3*-deficient mice. In addition, a cardiac sympathetic nerve retrograde tracer and a sympathectomy method were used to explore the relationship between sympathetic nerves and cardiac macrophages. We found that cardiac sympathetic nerves are significantly activated after ischemic stroke, which contributes to the infiltration of monocyte-derived macrophages and subsequent cardiac dysfunction.

CONCLUSIONS: Our findings suggest a potential pathogenesis of CCS involving the cardiac sympathetic nerve–monocyte-derived macrophage axis.

Key Words: cardiac dysfunction ■ ischemic stroke ■ monocyte-derived macrophage ■ NLRP3 inflammasome ■ sympathetic nerve

Cerebral-cardiac syndrome (CCS) refers to the development of cardiac dysfunction after central nervous system injuries, such as ischemic stroke, intracerebral hemorrhage, traumatic brain injury, and stress.^{1,2} Ischemic stroke is the primary cause of CCS, with more than 90% of individuals with ischemic stroke experiencing adverse cardiac events.¹ CCS is mainly characterized by arrhythmia, heart failure, and even

cardiac arrest.³ Animal studies have also widely reported that experimental stroke induced cardiac dysfunction and cardiac myocyte death in vivo, ex vivo, and in vitro.^{4–6} Owing to its stealth and instability, CCS is recognized as the second leading cause of death in the poststroke stage.⁷ However, the pathogenesis of CCS remains unclear, resulting in a lack of specific therapies targeting the syndrome.

Correspondence to: Hong-Fei Zhang and Feng-Xian Li, Department of Anesthesiology, Zhujiang Hospital, Southern Medical University, NO. 253 Industrial Avenue, Guangzhou, Guangdong, China. Email: zhanghongfei@smu.edu.cn; lifengxian81@smu.edu.cn

This article was sent to Neel S. Singhal, MD, PhD, Associate Editor, for review by expert referees, editorial decision, and final disposition.

Supplemental Material is available at <https://www.ahajournals.org/doi/suppl/10.1161/JAHA.123.034731>

For Sources of Funding and Disclosures, see page 15.

© 2024 The Authors. Published on behalf of the American Heart Association, Inc., by Wiley. This is an open access article under the terms of the [Creative Commons Attribution-NonCommercial-NoDerivs](https://creativecommons.org/licenses/by-nc-nd/4.0/) License, which permits use and distribution in any medium, provided the original work is properly cited, the use is non-commercial and no modifications or adaptations are made.

JAHA is available at: www.ahajournals.org/journal/jaha

CLINICAL PERSPECTIVE

What Is New?

- Cardiac monocyte-derived macrophage subset expansion aggravated the cardiac dysfunction in the context of ischemic stroke.
- Overactivation of the sympathetic nervous system recruited the cardiac macrophage after ischemic stroke.

What Are the Clinical Implications?

- Cardiac dysfunction after stroke is recognized as the second leading cause of death in the post-stroke stage. The present study may support that inhibiting excessive sympathetic nervous system activation and cardiac monocyte-derived macrophage subset expansion may be a potential approach for clinical treatment of cardiac dysfunction after stroke.

Nonstandard Abbreviations and Acronyms

CCR2	C-C chemokine receptor type 2
CCS	cerebral-cardiac syndrome
LVFS	left ventricular fractional shortening
MCA	middle cerebral artery
MCAO	middle cerebral artery occlusion
NLRP3	NOD-like receptor thermal protein domain associated protein 3
SCG	superior cervical ganglion

Inflammatory responses have been reported as a vital pathogenic mechanism of CCS.¹ Of note, immune cells play crucial roles in maintaining cardiac function and regulating the pathological process following cardiovascular disease. Macrophages, as dominant immune cells, have high heterogeneity and diversity. A previous study documented that CCS is characterized by macrophage expansion.⁸ Interestingly, cardiac macrophages can be divided into 2 distinct subsets: cardiac resident macrophages and monocyte-derived macrophages.⁹ The cardiac macrophage subset can be discriminated according to the expression of C-X3-C motif chemokine receptor 1 (CX3CR1) in resident macrophages and C-C chemokine receptor type 2 (CCR2) in monocyte-derived macrophages.^{10,11} Emerging evidence indicates that resident cardiac macrophages play fundamental roles in visceral coronary artery development, cardiomyocyte proliferation and maturation, cardiac electrical conduction, metabolic stability, inflammation control, and tissue remodeling.^{10,12,13} Cardiac monocyte-derived macrophages mediate

myocardial injury, fibrosis, and adverse heart remodeling and contribute to heart failure.^{14–16} However, the origin and function of cardiac macrophages in CCS remain unclear.

The cardiac nervous system plays a vital role in regulating both the physiological function and pathological progression of the heart. Hyperactivation of the sympathetic nervous system is a leading hypothesis about the mechanism of CCS.¹⁷ Interestingly, cardiac macrophages express alpha- and beta-adrenergic receptors, which can bind with norepinephrine, thereby regulating the inflammatory state of macrophages.¹⁸ The sympathetic nervous system has been widely reported to regulate macrophage function in various tissues, including bone marrow, gut, and white adipose tissue.^{19–21} However, whether the sympathetic nervous system regulates cardiac macrophages in ischemic stroke remains unknown.

In this study, we performed an ischemic stroke mouse model through middle cerebral artery occlusion (MCAO). CCS phenotype was induced after MCAO, which characterized by reduced cardiac systolic function, prolonged QT interval, and robust cardiac macrophage infiltration. To understand the source and function of cardiac macrophages after ischemic stroke, we used a transgenic mouse line and pharmacological methods to examine the components of cardiac macrophage subsets. Our results revealed that cardiac macrophage expansion in CCS predominantly involves monocyte-derived macrophages. Additionally, we found that NLRP3 (NOD [nucleotide oligomerization domain]-like receptor thermal protein domain associated protein 3) inflammasome activation may be a molecular target of monocyte-derived macrophage-induced cardiac dysfunction after stroke. Furthermore, through a combination of a genetic mouse model, retrograde nerve tracing, sympathectomy, and pharmaceutical inhibition, we demonstrated that cardiac sympathetic hyperactivation after ischemic stroke induces macrophage expansion in the heart, resulting in cardiac dysfunction. Overall, our study highlighted the important role of sympathetic nerve-induced cardiac monocyte-derived macrophages in CCS. These findings have implications for the development of targeted therapies, which focus on the interplay between the sympathetic nervous system and monocyte-derived macrophages in CCS.

METHODS

Animal

Our study examined male mice because male animals exhibited less variability in ischemic stroke phenotype. Male C57BL/6J mice (8–12 weeks) were acquired from Guangdong Sja Biotechnology Co. Ltd.

Cx3cr1^{GFP}Ccr2^{RFP} mice (Stock #: 032127), *Nlrp3^{-/-}* mice (Stock #: 021302), *Th^{cre}* mice (Stock #: 008601), and *ROSA26^{tdTomato}* mice (Stock #: 007909) were ordered from the Jackson Laboratory. All mice were of the C57BL/6J background, but only male transgenic mice were used for subsequent experiments. Mice were bred and housed in the Laboratory Animal Center of Zhujiang Hospital of Southern Medical University. All mice were allowed free access to food and water on a 12-hour light/dark cycle. All mice were grouped randomly, and a blind test was conducted in the animal experimental procedures.

Study Approval

All experiments were performed following the National Institutes of Health *Guide for the Care and Use of Laboratory Animals*. Experiments involving mice and protocols were performed according to protocols approved by the Medical Faculty Ethics Committee of Zhujiang Hospital, Southern Medical University (LAEC-2021-074, Guangdong, China).

Ischemic Stroke Mouse Model

The ischemic stroke mouse model was performed using MCAO, according to the protocol of our previous study.⁶ Briefly, mice were anesthetized with 2% isoflurane (RWD Life Science Co., Ltd, Shenzhen, China). After making a skin incision of the midline neck, a nylon monofilament with a blunted tip (Sebiona Technology Co. Ltd., Guangzhou, China) was inserted into the origin of the right middle cerebral artery (MCA) through the right external carotid artery to block the MCA blood. The suture remained in place for 1 hour without anesthesia, and reperfusion was followed by withdrawing the suture under anesthesia with 2% isoflurane. Mice were considered as ischemic stroke models when the MCA blood flow was reduced by more than 70% due to occlusion, which were included in further analyses. Mice that died during surgery were excluded. Sham-operated mice underwent the same procedure without inserting the monofilament.

Statistical Analysis

Animal numbers were determined based on our pilot experiments by power analysis using G power software (G power software 3.1.9.7, Germany).²² The required sample size needed to achieve a power of 80% with an alpha error of 0.05 was 4 to 10 animals for each experiment. Data were presented as the mean±SD and were analyzed using SPSS Statistic software (version 27, IBM, Chicago, IL). Normality of the data was tested using Shapiro–Wilk test. Based on normality test, Mann–Whitney *U* test or 2-sided Student *t* test was performed to determine significance, which was set

at $P<0.05$. For more than 2 arms comparison, 1-way ANOVA with Tukey's post hoc correction or Kruskal–Wallis H test was used, as appropriate. The difference between the groups was considered statistically significant at $P<0.05$.

A detailed description of the experimental procedures is provided in the Data S1. The antibodies and primers used in this study are listed in Tables S1 and S2. The data sets generated during or analyzed during the current study are available from the corresponding author upon reasonable request.

RESULTS

Cardiac Dysfunction Induced by Ischemic Stroke

Ischemic stroke is characterized by a reduced blood supply to brain tissue. We first performed the MCAO mouse model and confirmed it by laser speckle contrast imaging. We found that the right cerebral blood flow obviously decreased (up to 70%) during occlusion in the MCAO group (Figure 1A and 1B). Furthermore, we observed a substantial infarct area in the brain by 2,3,5-triphenyl tetrazolium chloride staining at 3 days after MCAO (Figure 1C) and notable brain atrophy at 28 days after MCAO (Figure 1D). These results indicate that the MCAO mouse model has the potential to replicate ischemic stroke.

Echocardiography and ECG are most used to evaluate cardiac function in mice in vivo.^{6,23} Prolongation of the QT interval is a risk factor for fatal arrhythmias.²⁴ The mice consistently exhibited prolonged QT and QTc intervals at 3 and 28 days post-MCAO treatment, compared with the sham group (Figure 1E and 1F). In addition, compared with the sham group, significantly decreased left ventricular ejection fraction (LVEF) and fractional shortening (LVFS) were demonstrated at 28 days, but no significant difference was found at 3 days in the MCAO group (Figure 1G and 1H). Collectively, these findings suggest that the experimental stroke model (MCAO) successfully induced cardiac dysfunction similar to that observed in human patients.

Ischemic Stroke Recruited Monocyte-Derived Macrophages Into the Heart

Myocardial inflammation plays an important role in CCS. To evaluate the change of immune cell clusters in response to ischemic stroke, we first performed flow cytometry on cardiac single cells isolated from sham or MCAO mice 3 days after the procedure. Cardiac macrophages and neutrophils were elevated in MCAO mice compared with sham mice (Figure S1A and S1B). However, no differences were found in B cells, T cells,

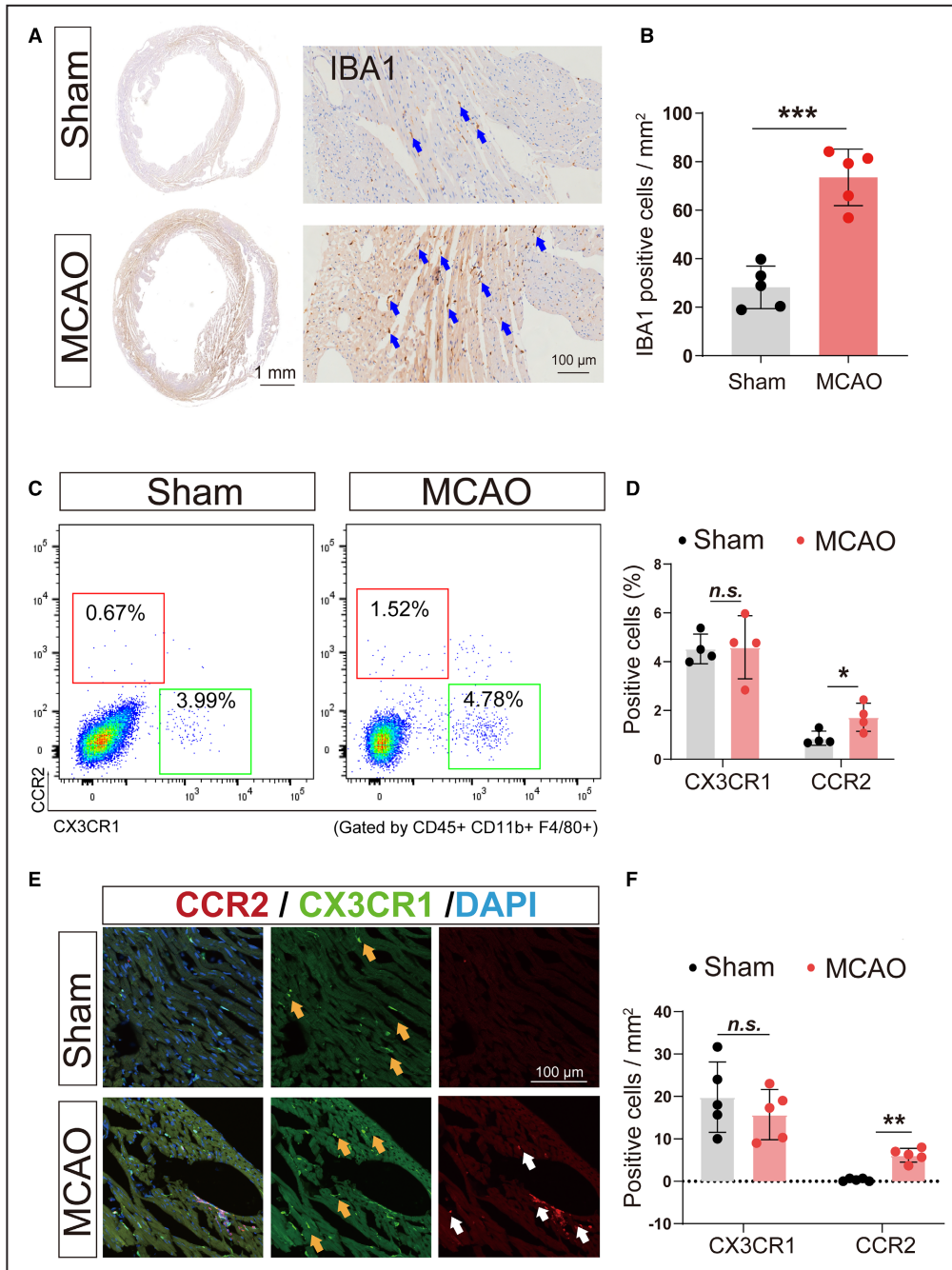


Figure 2. Cardiac macrophage subset altered after ischemic stroke.

A, Increased cardiac macrophages (blue arrow) in cardiac cross-sectional sections are indicated by IBA1 immunohistochemical staining. Scale bar: 1 mm and 100 μ m. **B**, Quantification of cardiac macrophages in the sham and MCAO groups (n=5 in each group, $P=0.0007$); the y axis represents the IBA1-positive cell number. Each dot represents the mean IBA1-positive cell number of 4 different fields of view in each slice of the heart. **C**, Representative flow cytometry plots of resident macrophages (green frame) and monocyte-driven macrophages (red frame). **D**, Quantification of resident-(CX3CR1⁺, $P=0.9306$) and monocyte-derived macrophages (CCR2⁺, $P=0.0369$) in the sham and MCAO groups (n=4 in each group). **E**, Representative immunofluorescence images of resident- (yellow arrow) and monocyte-driven macrophages (white arrow) in cross-sectional sections of the heart. Green: CX3CR1; Red: CCR2. Scale bar: 100 μ m. **F**, Quantification of CX3CR1⁺ ($P=0.3908$) and CCR2⁺ ($P=0.0025$) in the sham and MCAO groups (n=5 in each group). The y axis represents the number of CX3CR1⁺- or CCR2⁺-positive cells. Each dot represents the mean number of positive cells in 3 different fields of view in each slice of the heart. CCR2 indicates C-C chemokine receptor type 2; CX3CR1, C-X3-C motif chemokine receptor 1; IBA1, ionized calcium binding adaptor molecule 1; MCAO, middle cerebral artery occlusion; and n.s., not significant. * $P<0.05$, ** $P<0.01$.

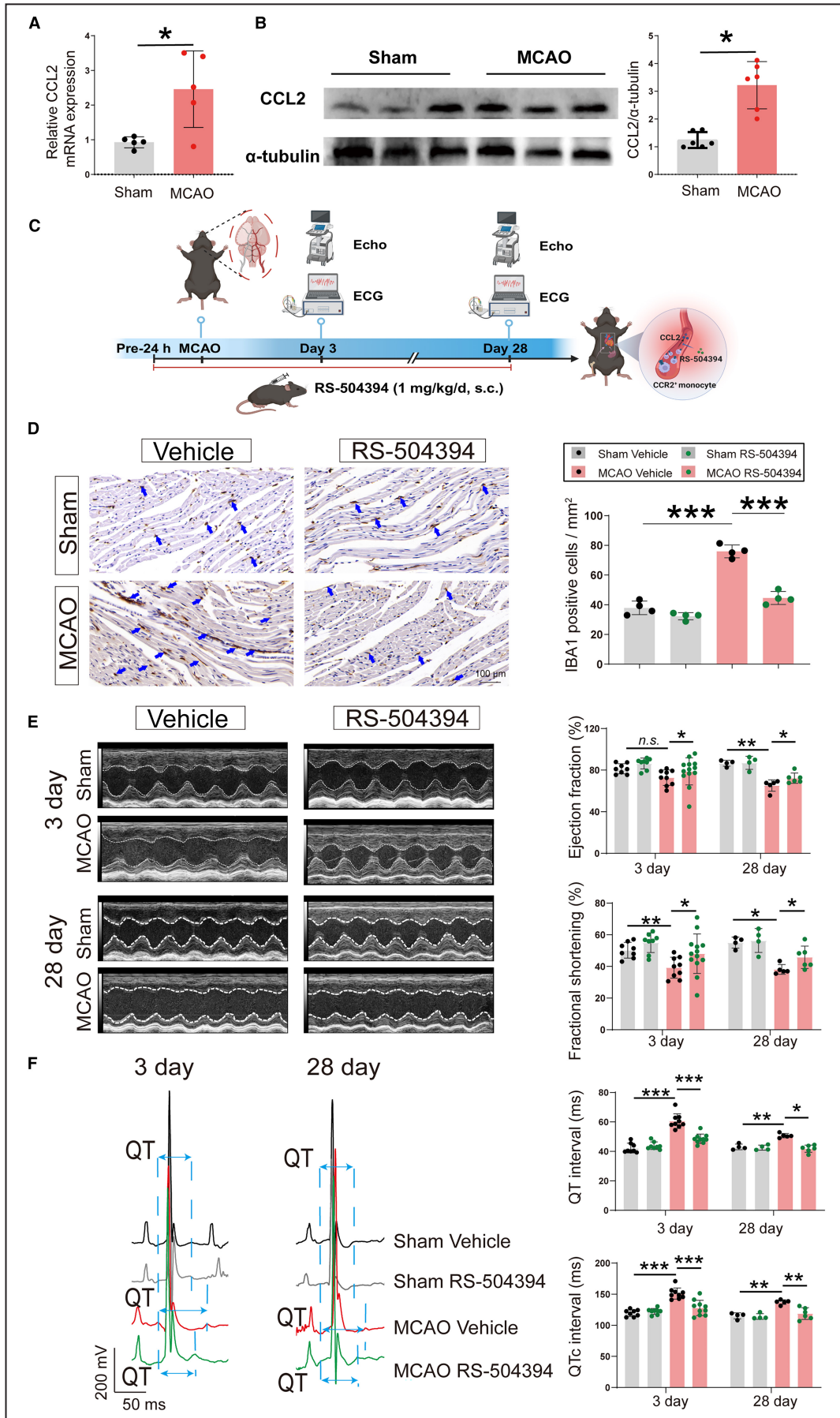


Figure 3. Pharmacological inhibition of CCR2⁺ monocyte-derived macrophages ameliorated ischemic stroke-induced cardiac dysfunction.

A, Quantification of cardiac CCL2 mRNA expression level in the sham and MCAO groups (n=5 in each group, $P=0.0110$). **B**, CCL2 protein of myocardial tissue is indicated by Western blot and quantification in the sham and MCAO groups (n=6 in each group, $P=0.0303$). **C**, Schematic diagram of RS-504394 treatment to inhibit CCR2⁺ monocyte-derived macrophages in vivo. Mice received RS-504394 (1 mg/kg) once a day 24 hours before the MCAO or sham procedure. **D**, Representative IBA1 immunohistochemical staining of cardiac macrophages (blue arrow) in cardiac cross-sectional section. Scale bar: 100 μm . Quantification of cardiac macrophages in the sham and MCAO groups with vehicle or RS-504394 treatment (n=4 in each group, $P<0.0001$ and $P<0.0001$). The y axis represents the IBA1-positive cell number. Each dot represents the mean IBA1-positive cell number of four different fields of view in each slice of the heart. **E**, Representative echocardiography frames and quantification of the LVEF and LVFS on day 3 (n=8–13 in each group) and day 28 (n=4–6 in each group) in the sham and MCAO groups with vehicle or RS-504394 treatment. **F**, Representative ECG monitoring image and quantification of the QT and QTc intervals on day 3 (n=8–10 in each group) and day 28 (n=4–6 in each group) in the sham and MCAO groups with vehicle or RS-504394 treatment. CCL2 indicates chemokine ligand 2; CCR2, C-C chemokine receptor type 2; Echo, echocardiography; IBA1, ionized calcium binding adaptor molecule 1; LVEF, left ventricular ejection fraction; LVFS, left ventricular fractional shortening; MCAO, middle cerebral artery occlusion; n.s., not significant; and s.c., subcutaneous injection. * $P<0.05$, ** $P<0.01$, *** $P<0.001$.

and dendritic cell clusters in the heart (Figure S1B). Similarly, we found that IBA1 (ionized calcium binding adaptor molecule 1)-positive cells were increased in the heart sections of MCAO mice (Figure 2A and 2B). Interestingly, correlation analysis revealed a negative relationship between the percentage of cardiac macrophages (counted by flow cytometry) and the LVEF of the heart in both MCAO and sham mice (Figure S1C and S1D). These results suggest that cardiac macrophage expansion after ischemic stroke onset may contribute to cardiac dysfunction.

Cardiac macrophages display obvious heterogeneity and can be divided into resident macrophages and monocyte-derived macrophages.¹⁰ *Cx3cr1^{GFP}Ccr2^{RFP}* reporter mice have been widely used to distinguish resident macrophages (C-X3-C motif chemokine receptor 1⁺) and monocyte-derived macrophages (CCR2⁺) lineages.^{25,26} Given the large increase in cardiac macrophage abundance following ischemic stroke, we used *Cx3cr1^{GFP}Ccr2^{RFP}* mice to further explore the subset population of increased cardiac macrophages. In response to ischemic stroke stimulation, cardiac CCR2⁺ macrophages, except for C-X3-C motif chemokine receptor 1⁺ macrophages, were significantly increased in MCAO mice (Figure 2C and 2D). A significant increase in CCR2⁺ positive cells was likewise found in the heart sections of the MCAO mice (Figure 2E and 2F). Resident macrophages renew through self-proliferation, and Ki-67 is a marker of cell proliferation.²⁷ Surprisingly, there were no significant differences in cardiac Ki-67⁺ macrophages between MCAO mice and sham mice (Figure S1E and S1F). Taken together, these results suggest that monocyte-derived macrophages are the dominant subset for cardiac macrophage expansion after ischemic stroke.

The CCL2–CCR2 Axis Is Responsible for Cardiac Dysfunction After Stroke

CCL2 (chemokine ligand 2) is the key chemokine for recruiting CCR2⁺ monocyte infiltration.²⁸ Therefore,

we evaluated the mRNA and protein expression levels of CCL2 in the heart after ischemic stroke. As anticipated, the expression of CCL2 mRNA and protein was significantly increased in the MCAO group (Figure 3A and 3B). RS-504394 is an efficient CCR2 antagonist that inhibits the recruitment of CCR2⁺ monocytes.²⁹ To explore the role of the CCL2–CCR2 axis in CCS, RS-504394 was pretreated 24 hours before the MCAO or sham procedure and was applied once a day for 28 days after the surgery (Figure 3C). We found that RS-504394 treatment reduced cardiac macrophage expansion after stroke (Figure 3D). Furthermore, RS-504394 treatment sufficiently restored cardiac function, which shows improved LVEF and LVFS at 28 days (Figure 3E) and shortening QT and QTc intervals at 3 and 28 days (Figure 3F) after ischemic stroke. These results identify the crucial role of the CCL2–CCR2 axis in cardiac macrophage expansion and cardiac dysfunction after ischemic stroke.

Monocyte-Derived Macrophages Displayed a Proinflammatory Profile in CCS

Different cardiac macrophage subsets play distinct roles in the cardiac pathological process.³⁰ To probe the spectrum of gene expression profiles and function among cardiac macrophage subsets in CCS, we established the MCAO mouse model using *Cx3cr1^{GFP}Ccr2^{RFP}* mice. Subsequently, fluorescence-activated cell sorting was used to separate and collect cardiac resident (18239 \pm 10629) and monocyte-derived macrophages (4380 \pm 1693) for Smart-seq2 RNA sequencing at 3 days after MCAO (Figure 4A and 4B). There were 2456 genes of different levels in monocyte-derived macrophages, of which 1301 were upregulated genes and 1155 were downregulated genes, compared with those in resident macrophages (Figure 4C). Further analysis of the gene expression pattern in both cardiac macrophage subsets. We found that cardiac monocyte-derived macrophages expressed high levels of proinflammatory

response genes, such as *IL6*, *JAK2*, and *MMP9*. The resident macrophages were also characterized by high expression of anti-inflammatory response-related genes, such as *IGF1*, *TLR2*, and *TREM2* (Figure 4D). As previously reported, macrophages can be divided into classic inflammatory polarization (M1) and alternatively activated polarization (M2).³¹ Of note, cardiac monocyte-derived macrophages are characterized by the high expression of *IL1 β* , *IL6*, and *IL12*, which resemble the signatures of M1 macrophages. Moreover, resident macrophages express high levels of M2-related genes, such as *IL10*, *CD163*, and *TGF β* (Figure 4D and Figure S2A).

Gene Ontology analysis with differentially expressed genes was also performed in both cardiac macrophage subsets. In Gene Ontology terms, differentially expressed genes were enriched in the immune system process, inflammatory response, adaptive immune response, and immune response (Figure 4E), indicating the inflammatory activation status of monocyte-derived macrophages. Differentially expressed genes also presented enrichment in protein binding, cytokine activity, signaling receptor binding, plasma membrane, and intracellular membrane-bound organelle of cellular component and molecular function in Gene Ontology terms (Figure S2B and S2C). The analysis of Kyoto Encyclopedia of Genes and Genomes pathways by differentially expressed genes showed enrichment in cytokine–cytokine receptor interaction, metabolic pathways, and chemokine signaling pathways (Figure S2D). Collectively, these data suggest that cardiac monocyte-derived macrophages demonstrate a significant proinflammatory pattern in CCS.

NLRP3 Inflammasome Activation Contributed to Cardiac Dysfunction After Stroke

We next sought to explore the functional characteristics of monocyte-derived macrophages in the context of inflammation in CCS. Of note, the activation of the NLRP3 inflammasome is the key component in inflammatory cascade.³² The NLRP3 inflammasome activation-related genes *NLRP3*, *ASC*, *IL1 β* , and *NF κ B* were upregulated in monocyte-derived macrophages relative to resident macrophages, as indicated by Smart-seq2 RNA sequencing (Figure 5A). We further confirmed a substantial increase in the mRNA expression of NLRP3 inflammasome activation-related genes in the heart tissue of MCAO mice (Figure 5B). These results indicated that the NLRP3 inflammasome was activated in the heart after stroke.

Furthermore, we used both *Nlrp3*^{-/-} and wild-type mice to establish the MCAO mode. We found that the LVEF and LVFS were significantly increased at 28 days after the MCAO procedure in *Nlrp3*^{-/-} mice compared

with wild-type mice (Figure 5C). Similarly, the QT and QTc intervals were preserved at 3 and 28 days after MCAO in *Nlrp3*^{-/-} mice (Figure 5D). Interestingly, we found that cardiac macrophages were decreased in *Nlrp3*^{-/-} mice compared with wild-type mice after MCAO procedure (Figure 5E). Collectively, these results reveal that NLRP3 inflammasome activation may be a molecular target of cardiac monocyte-derived macrophage-induced cardiac dysfunction after ischemic stroke.

Cardiac Sympathetic Activation Presented After Stroke

Cardiovascular diseases are characterized in part by an imbalance in autonomic nervous system activation, which also contributes to regulating cardiac inflammation. Tyrosine hydroxylase is used to label the cell bodies and nerve terminals of sympathetic neurons.³³ To determine sympathetic nerve activation in the heart after ischemic stroke, we used the Cre/LoxP recombination system to cross the *Th*^{Cre/+} and *ROSA26*^{tdTomato/+} mice and thus generated *Th*^{tdTomato} mice, in which the sympathetic nerve is selectively expressed as a red fluorescent protein reporter (tdTomato) (Figure 6A). Furthermore, WGA-AF488, an efficient retrograde fluorescent neural tracer, was injected into the myocardium of *Th*^{tdTomato} mice via echocardiography guidance³⁴ (Figure 6B, Video S1). Seven days after intramyocardial injections, WGA-488 could be found in the left ventricle myocardium, indicating the success of intramyocardial injection (Figure 6C). Retrograded WGA-AF488 was likewise found in tdTomato⁺ neurons in the superior cervical ganglion (SCG) (Figure 6D), suggesting that SCG sympathetic neurons project nerve fibers to the heart.

C-fos and pERK were used as markers for neuron activation.³⁵ We found that C-fos- and pERK-positive cells were increased in the SCG in MCAO mice compared with sham mice (Figure 6E, Figure S3A). In addition, norepinephrine was found to be significantly evoked in the serum after MCAO (Figure 6F). The ratio of low-frequency power to high-frequency power in heart rate variability can directly reflect sympathetic nerve activity. Similarly, low-frequency power to high-frequency power was significantly enhanced in MCAO mice compared with sham mice (Figure 6G). Collectively, these results indicate that cardiac sympathetic nerves are characterized by excess activation after ischemic stroke.

Sympathetic Activation Induced Cardiac Macrophage Expansion After Stroke

Neural activity can directly regulate macrophage recruitment and infiltration. We found that cardiac macrophages primarily localize into clusters along the cardiac sympathetic nerve fibers following MCAO

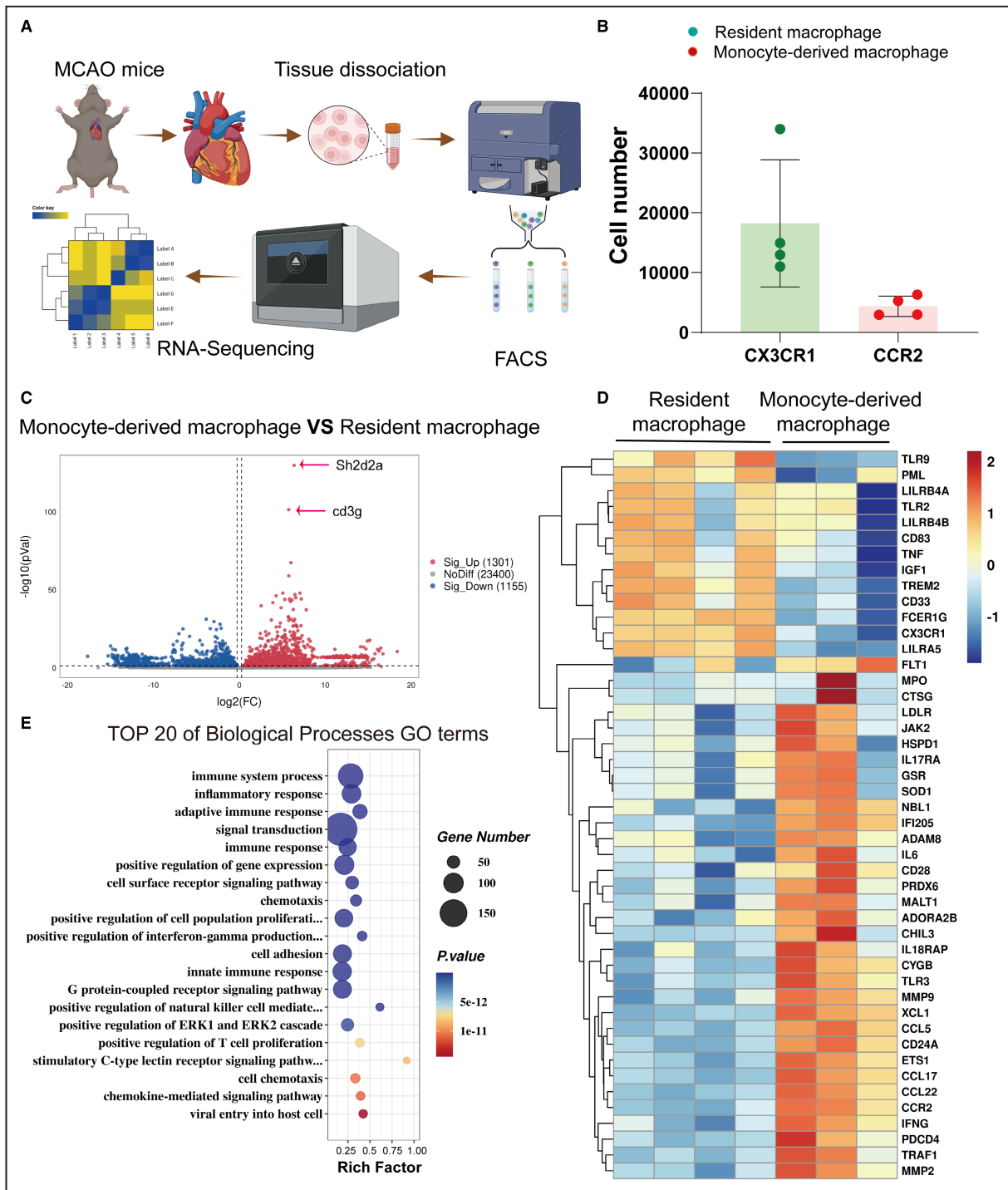


Figure 4. RNA sequencing of the cardiac macrophage subset during CCS progression.

A, The schematic diagram indicates that the mice were subjected to the MCAO procedure, and then hearts were collected for FACS sorting. All resident macrophages and monocyte-derived macrophages of each mouse heart were collected for Smart-seq2 RNA sequencing. **B**, The cell number of FACS-sorted cardiac macrophages. Each dot represents the cardiac macrophages from a mouse. Red: monocyte-derived macrophage; Green: resident macrophage. **C**, Volcano plot showing the differentially expressed genes between cardiac monocyte-derived macrophages and resident macrophages in MCAO mice. Red: upregulated genes, blue: downregulated genes, gray: unchanged genes. RNA sequencing analysis with the parameters of $P < 0.05$ and absolute fold change ≥ 1.2 were considered differentially expressed genes. **D**, Heat map of differentially expressed anti- and proinflammatory genes between different cardiac macrophage subsets in MCAO mice. **E**, GO enrichment analysis of cardiac monocyte-derived macrophages and resident macrophages. The y axis represents the GO pathways, and the x axis represents the rich factor. CCS indicates cerebral-cardiac syndrome; FACS, fluorescence-activated cell sorting; GO, Gene Ontology; and MCAO, middle cerebral artery occlusion.

(Figure 7A), suggesting that sympathetic nerves may participate directly in cardiac macrophage infiltration. To further investigate the role of sympathetic nerves in regulating cardiac macrophage expansion, we performed SCG resection 7 days before the MCAO or sham procedure (Figure 7B). Interestingly, compared with the control group (MCAO without SCG resection), SCG resection significantly reduced cardiac macrophage infiltration after stroke (Figure 7C). SCG resection also elevated the LVEF and LVFS as well as decreased the QT and QTc intervals after MCAO (Figure 7D and 7E). Furthermore, mice were treated with propranolol for pharmacologically inhibiting the function of norepinephrine for 28 days after stroke onset (Figure S4A). Compared with the vehicle treatment group, cardiac macrophage expansion was reversed in the propranolol treatment group after stroke (Figure S4B). Additionally, we found that propranolol treatment protected cardiac function after stroke, which manifested as increased LVEF and LVFS as well as decreased QT and QTc intervals (Figure S4C and S4D). Together, these results demonstrate that sympathetic activation induces cardiac macrophage expansion, resulting in cardiac dysfunction after stroke.

DISCUSSION

In this study, we highlighted the vital role of cardiac monocyte-derived macrophages in CCS. The significant expansion of the cardiac monocyte-derived macrophage subset coincided with cardiac dysfunction in the context of ischemic stroke. Of note, we found that monocyte-derived macrophages had a proinflammatory profile. NLRP3 inflammasome activation may be a potential target in monocyte-derived macrophages expansion, which induces cardiac dysfunction after stroke. In addition, the activation of cardiac sympathetic nerves from SCG after stroke coincided with the expansion of cardiac macrophages. SCG resection and propranolol treatment prevented cardiac dysfunction after stroke by inhibiting cardiac macrophage recruitment. Our study revealed that inhibiting the expansion of the cardiac monocyte-derived macrophage

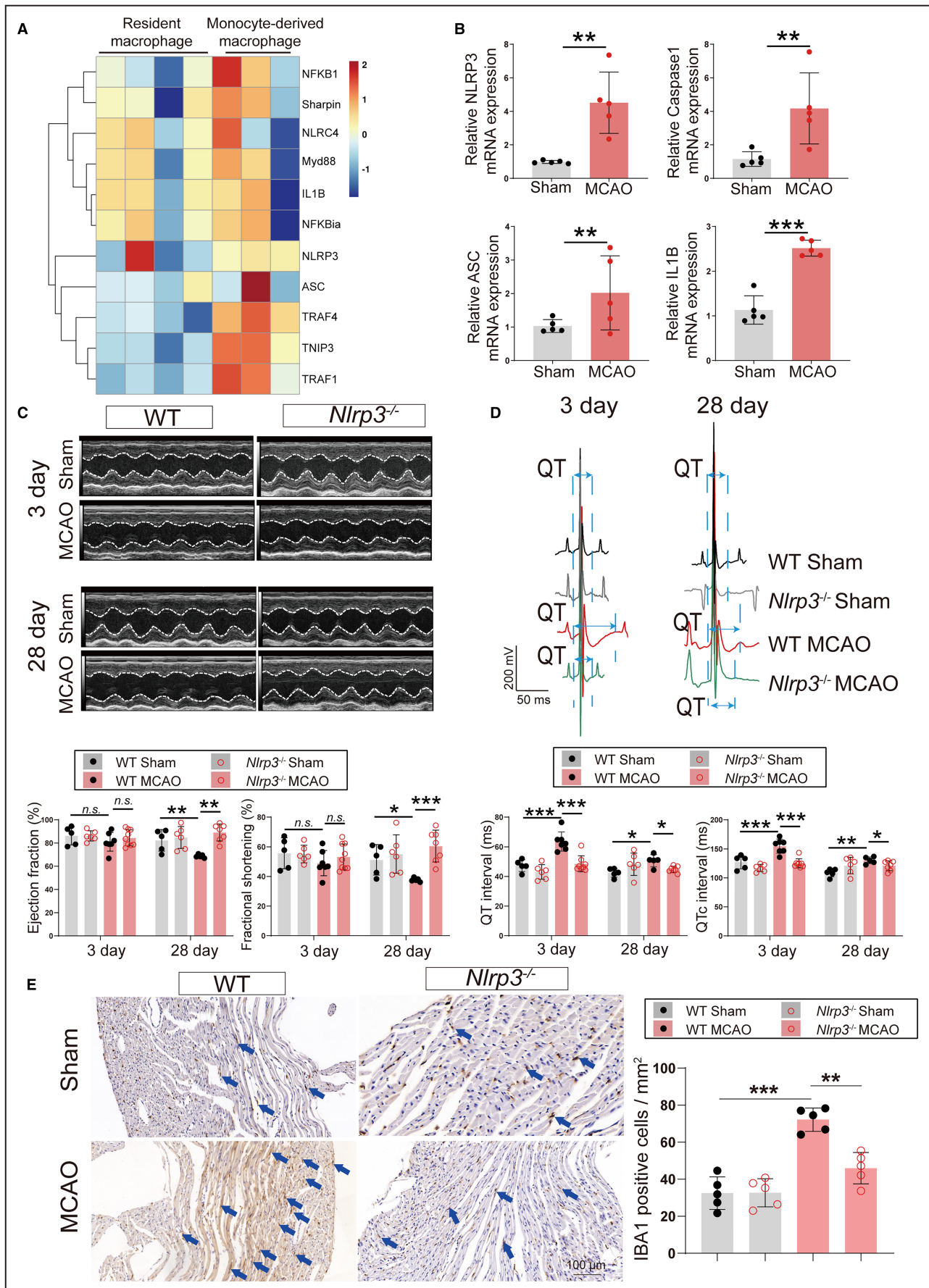
subset by harnessing the sympathetic nerve could be a potential therapeutic strategy for cardiac dysfunction after stroke in clinical settings.

The most common complication after ischemic stroke is cardiac related, with an estimated occurrence of approximately 20% to 90% in clinical settings.^{36–38} Cardiac complications after ischemic stroke also indicate a higher risk of mortality in the poststroke stage.⁷ Of note, arrhythmia is the most prevalent cardiac complication in ischemic stroke, with a prevalence of 74.4% within 24 hours following stroke onset.³⁹ Surprisingly, we identified that QT and QTc intervals were prolonged at 3 and 28 days, respectively, after ischemic stroke. The morbidity of left ventricular systolic dysfunction after ischemic stroke is up to 11.6%.⁴⁰ Alexandre et al found that experimental ischemic stroke-induced reduction of LVFS in vivo and of left ventricle developed pressure ex vivo in isolated perfused hearts.⁴ However, the evaluation of cardiac function ex vivo in isolated perfused hearts failed to detect the influence of the nervous system and the immune system in the pathological progression of CCS. Therefore, we mainly used echocardiography and ECG in vivo to evaluate the cardiac function of mice in the present study. We also found decreased LVEF and LVFS in ischemic stroke mice at 28 days postoperation.

Macrophages, as one of the most important immune cell subsets in the heart, are involved in cardiac inflammation, efferocytosis, tissue remodeling, and homeostasis. An increasing number of studies have highlighted that under homeostatic conditions, cardiac resident macrophages mainly take part in cardiac electrical conduction and metabolic stability and promote cardiac recovery after cardiac injury.^{11,41,42} In contrast, monocyte-derived macrophages are recruited and expanded during myocardial injury, which plays a vital role in producing inflammatory cytokines, promoting myocardial fibrosis, and contributing to adverse remodeling.^{10,14–16} CCR2⁺ cardiac macrophage abundance is predictive of poor prognosis in patients with heart failure.¹³ In this study, we found that CCR2⁺ cardiac macrophages were increased in the heart after ischemic stroke, which also corresponds to cardiac dysfunction, suggesting the essential role of

Figure 5. NLRP3 inflammasome activation in the heart contributed to CCS.

A, Heat map of NLRP3 inflammasome activation-related genes expression from Smart-seq2 RNA sequencing in MCAO mice. Red: upregulated genes, blue: downregulated genes. **B**, Quantification of *NLRP3*, *ASC*, *Caspase1*, and *IL1 β* mRNA expression levels in the heart in the sham and MCAO groups (n=5 in each group, $P=0.0026$, $P=0.0080$, $P=0.0014$, and $P=0.0001$). **C**, Representative echocardiography frames and quantification of the LVEF and LVFS on day 3 and day 28 in the sham and MCAO groups of WT or *Nlrp3*^{-/-} mice (n=5–9 in each group). **D**, Representative ECG monitoring image and quantification of the QT and QTc intervals on day 3 and day 28 in the sham and MCAO groups of WT or *Nlrp3*^{-/-} mice (n=5–8 in each group). **E**, Representative IBA1 immunohistochemical staining of cardiac macrophages (blue arrow) in cardiac cross-sectional section. Scale bar: 100 μ m. Quantification of cardiac macrophages in the sham and MCAO groups in WT or *Nlrp3*^{-/-} mice (n=5 in each group, $P<0.0001$ and $P=0.0036$). CCS indicates cerebral-cardiac syndrome; IBA1, ionized calcium binding adaptor molecule 1; LVEF, left ventricular ejection fraction; LVFS, left ventricular fractional shortening; MCAO, middle cerebral artery occlusion; NLRP3, NOD-like receptor thermal protein domain associated protein; n.s., not significant; and WT, wild type. * $P<0.05$, ** $P<0.01$, *** $P<0.001$.



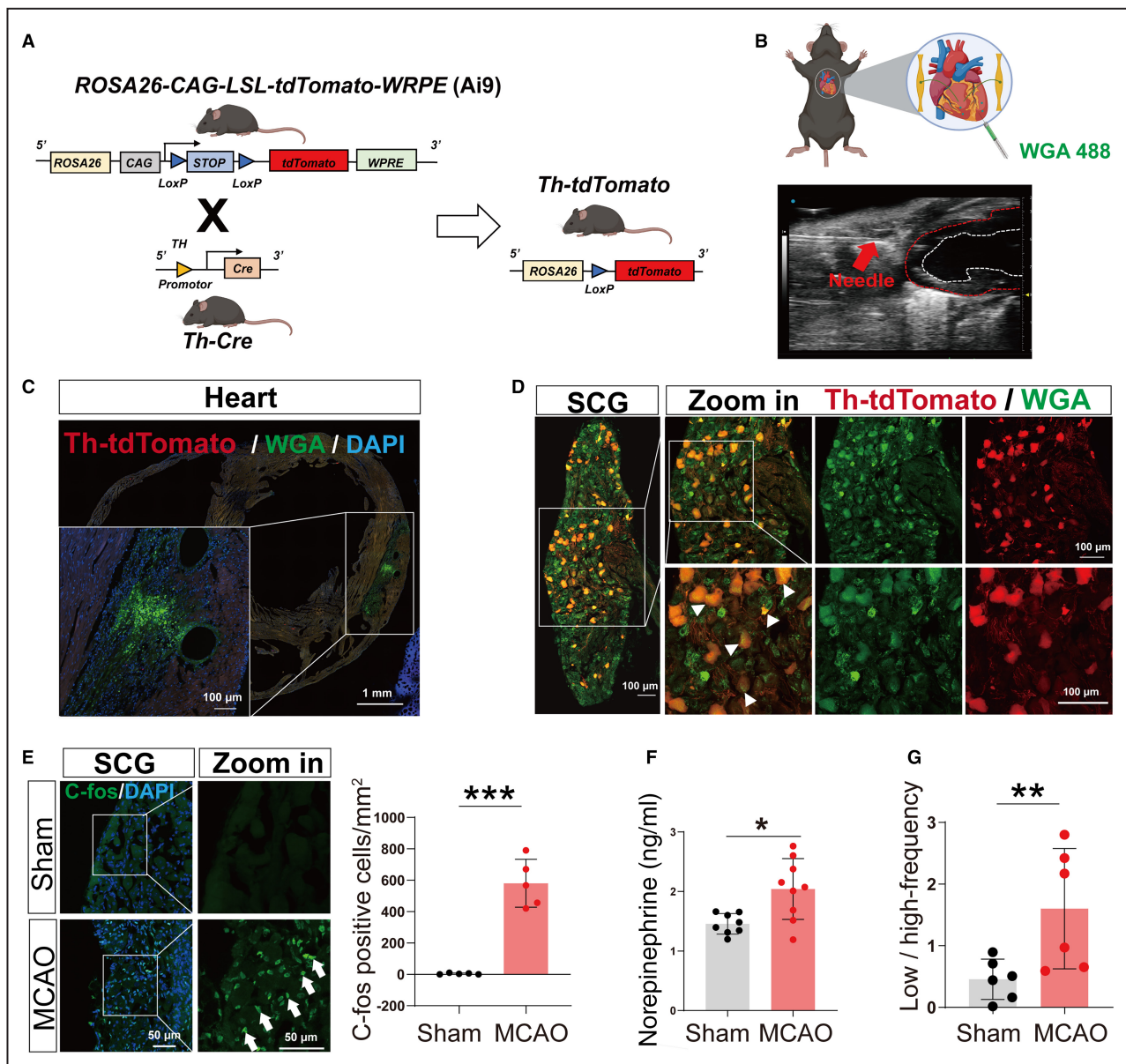


Figure 6. Cardiac sympathetic nerves from the superior cervical ganglion were activated after ischemic stroke.

A, Schematic diagram showing the generation of *Th^{tdTomato}* mice by crossing *Th^{Cre/+}* mice and *ROSA26^{tdTomato/+}* (Ai9) mice. **B**, Schematic diagram of intramyocardial WGA-488 injection for retrograde neural tracers in *Th^{tdTomato}* mice. Representative images of intramyocardial injections by using an ultrasound-guided transthoracic procedure. The red arrow indicates the needle. The red dashed area indicates the outer wall of the left ventricle, and the white dashed area indicates the inner wall of the left ventricle. **C**, Representative images of cardiac slices after intramyocardial WGA-488 injection. WGA-488 in the heart indicates a successful injection. Green: WGA-488; Red: tdTomato; Blue: DAPI. Scale bar: 100 μ m and 1 mm. **D**, Representative images of retrograde WGA-488 (green) in TH-positive cells (red, white arrow) in the SCG. Scale bar: 100 μ m. **E**, Representative images of activating neurons (white arrow) in the SCG with C-fos staining and quantification of the number of positive cells in sham and MCAO mice ($n=5$ in each group, $P=0.0001$). The y axis represents the number of C-fos-positive cells in the SCG. Each dot represents the mean number of positive cells in 3 different fields of view of each slice. Green: C-fos; Blue: DAPI. Scale bar: 50 μ m. **F**, Quantification of the level of norepinephrine in serum in sham ($n=8$) and MCAO mice ($n=9$, $P=0.0347$). **G**, Quantification of the ratio of low-frequency power to high-frequency power in heart rate variability in sham and MCAO mice ($n=6$ in each group, $P=0.0021$). MCAO indicates middle cerebral artery occlusion; SCG, superior cervical ganglion; and TH, tyrosine hydroxylase. * $P<0.05$, ** $P<0.01$, *** $P<0.001$.

monocyte-derived macrophages in promoting cardiac damage in ischemic stroke. The NLRP3 inflammasome is one of the most important members of the NLR receptor family, which is mainly expressed and activated

in macrophages. It can enhance the synthesis of proinflammatory cytokines by sensing intracellular signals, thereby causing inflammatory damage to tissues and organs.⁴³ We found that NLRP3 deficiency remarkably

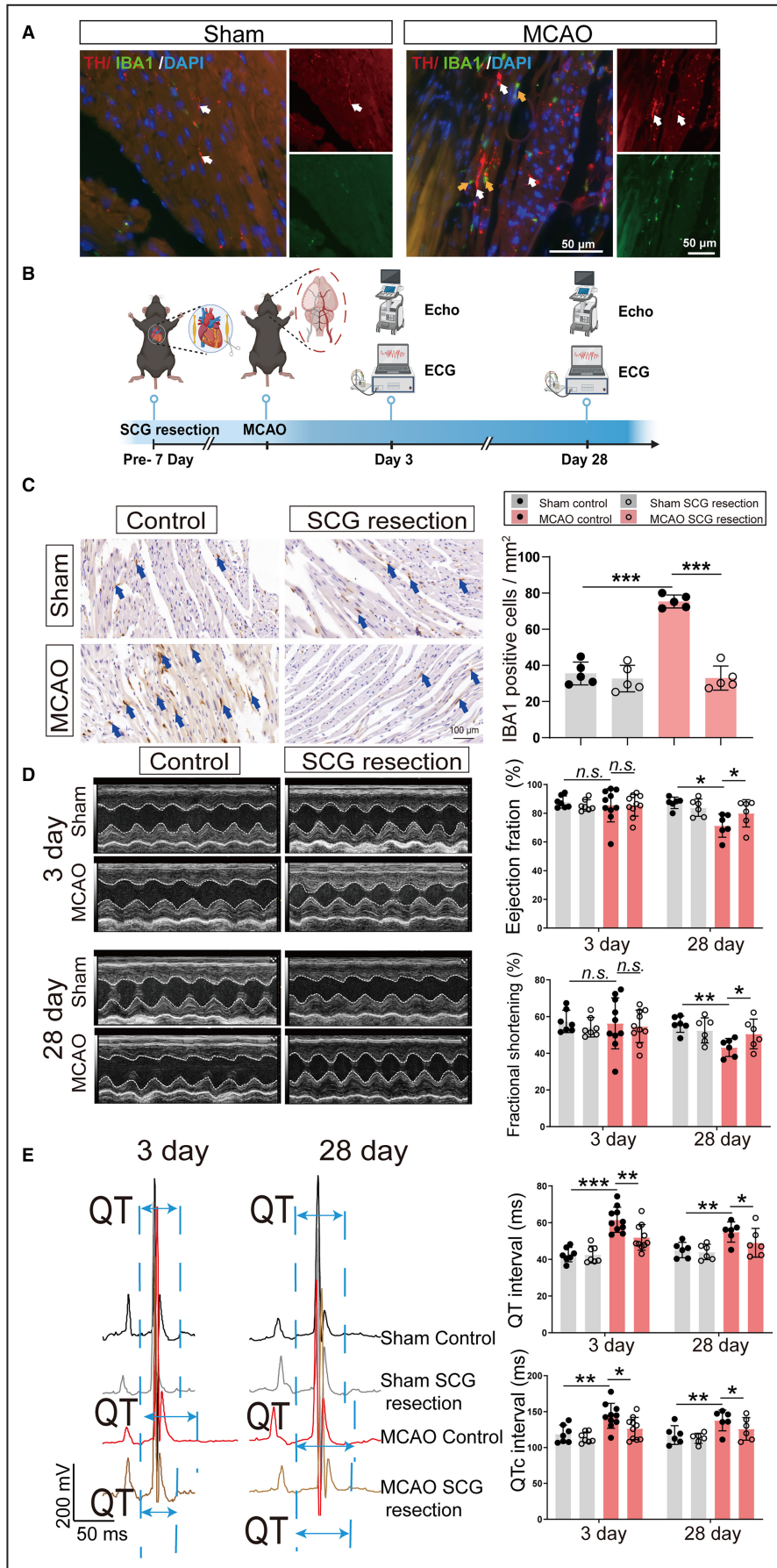


Figure 7. Cardiac sympathetic nerve activation recruited cardiac macrophage and induced cardiac dysfunction.

A, Representative images refer to the spatial relationship between cardiac macrophages (yellow arrow) and sympathetic nerve fibers (white arrow). Green: IBA1; Red: TH; Blue: DAPI. Scale bar: 50 μm . **B**, Schematic diagram indicating that SCG resection was performed at 7 days before the MCAO or sham procedure in mice. **C**, Representative IBA1 immunohistochemical staining of cardiac macrophages (blue arrow) in cardiac cross-section. Scale bar: 100 μm . Quantification of cardiac macrophages in the sham and MCAO groups with and without SCG resection ($n=5$ in each group, $P<0.0001$ and $P<0.0001$). The y axis represents the IBA1-positive cell number. Each dot represents the mean IBA1-positive cell number of 4 different fields of view in each slice of the heart. **D**, Representative echocardiography frames and quantification of the LVEF and LVFS on day 3 and day 28 in the sham and MCAO groups with and without SCG resection ($n=6-10$ in each group). **E**, Representative ECG monitoring image and quantification of the QT and QTc intervals on day 3 and day 28 in the sham and MCAO groups with and without SCG resection ($n=6-10$ in each group). IBA1 indicates ionized calcium binding adaptor molecule 1; LVEF, left ventricular ejection fraction; LVFS, left ventricular fractional shortening; MCAO, middle cerebral artery occlusion; n.s., not significant; and SCG, superior cervical ganglion. * $P<0.05$, ** $P<0.01$, *** $P<0.001$.

improved cardiac function after ischemic stroke. Our findings suggest that NLRP3 inflammasome activation plays an essential role in the development of cardiac dysfunction after ischemic stroke.

To date, prominent studies have reported the close relationship between the nervous system and the immune system, which is also called the neuroimmune interaction.^{44,45} A previous study has reported that the norepinephrine level in the heart is enhanced after stroke.¹⁷ However, cardiac norepinephrine primarily has 2 sources: the adrenal glands and the sympathetic nerves in the heart. In this study, we observed enhanced activation of sympathetic elements in the SCG that project to the heart after ischemic stroke. Our data strongly suggest that excessive cardiac sympathetic activation appears after stroke. Of note, sympathetic nerves have a significant regulatory effect on macrophages in cardiovascular disease.²⁷ The gastrointestinal tract reveals the presence of sympathetic nerve axons innervating macrophages in proximity to the nerves.^{19,20} Very much in line with these studies, we found that recruited macrophages in the heart tend to cluster around the sympathetic nerves, suggesting that the sympathetic nervous system may play an important role in cardiac macrophage recruitment after stroke. Importantly, we found that SCG resection and propranolol treatment inhibited cardiac macrophage expansion and prevented cardiac dysfunction after stroke, which provided targets for the development of CCS therapies in the clinic.

The limitation of this study is that we cannot precisely define a molecular mechanism of monocyte-derived macrophages in CCS pathogenesis. Our Smart-seq2 RNA sequencing data demonstrated only that NLRP3 inflammasome-related genes were highly expressed in the monocyte-derived macrophage subset. Similarly, NLRP3 inflammasome-related genes have been reported to be highly expressed in cardiac monocyte-derived macrophages during cardiac impairments, including myocardial infarction, dilated cardiomyopathy, and ischemic cardiomyopathy.^{10,13} However, we used global *NLRP3*-deficient mice only to demonstrate the role of NLRP3 in CCS in this study. To further explore the role of NLRP3 inflammasome activation in monocyte-derived macrophage subsets,

monocyte-derived macrophage-specific *NLRP3*-deficient mice would be a foundation for future studies.

Interestingly, our data demonstrated that inhibiting the infiltration of cardiac monocyte-derived macrophages could partly rescue the cardiac function after stroke, but the cardiac function did not return to normal levels. However, global *NLRP3*-deficient mice still maintained normal cardiac function levels after stroke, similar to wild-type sham mice, raising questions about the contribution of NLRP3 inflammasome in other cell types to post-MCAO cardiac function. Of note, we found that in addition to cardiac macrophages, neutrophils were another immune cell that was markedly increased in the heart after stroke. NLRP3 inflammasomes have been reported to have high expression and activation in neutrophils.⁴⁶ Therefore, the role of NLRP3 inflammasome activation in neutrophils in CCS also needs further studies.

CONCLUSIONS

In summary, our study revealed that the expansion of the cardiac monocyte-derived macrophage subset is induced by the high expression of *CCL2* in the heart after stroke. NLRP3 inflammasome activation may be a molecular target in cardiac monocyte-derived macrophage-induced cardiac inflammatory injury. Additionally, overactivation of the sympathetic nervous system after stroke has a direct regulatory effect on cardiac macrophage expansion. Our study highlights that inhibiting excessive sympathetic nervous system activation and cardiac monocyte-derived macrophage subset expansion may be a potential approach for clinical treatment of cardiac dysfunction after stroke.

ARTICLE INFORMATION

Received February 1, 2024; accepted March 25, 2024.

Affiliations

Department of Anesthesiology, Zhujiang Hospital, Southern Medical University, Guangzhou, Guangdong, China (H-B.L., P.H., M-Y.Y., Z-J.Y., Y-P.J., X-X.H., S-Y.X., F-X.L., H-F.Z.); and State Key Laboratory of Ophthalmology, Zhongshan Ophthalmic Center, Sun Yat-sen University, Guangdong Provincial Key Laboratory of Ophthalmology and Visual Science, Guangzhou, Guangdong, China (J-Y.Z.).

Sources of Funding

This work was supported by grant 82070526 (to H.-F.Z.) and grant 82271392 (to F.-X.L.) from the National Natural Science Foundation of China and grant 2021A151011652 (to H.-F.Z.) from the Natural Science Foundation of Guangdong Province, China.

Disclosures

None.

Supplemental Material

Data S1

Video S1

REFERENCES

- Lin H-B, Li F-X, Zhang J-Y, You Z-J, Xu SY, Liang W-B, Zhang H-F. Cerebral-cardiac syndrome and diabetes: cardiac damage after ischemic stroke in diabetic state. *Front Immunol*. 2021;12:737170. doi: [10.3389/fimmu.2021.737170](https://doi.org/10.3389/fimmu.2021.737170)
- Chen Z, Venkat P, Seyfried D, Chopp M, Yan T, Chen J. Brain-heart interaction: cardiac complications after stroke. *Circ Res*. 2017;121:451–468. doi: [10.1161/CIRCRESAHA.117.311170](https://doi.org/10.1161/CIRCRESAHA.117.311170)
- Taggart P, Critchley H, Lambiase PD. Heart-brain interactions in cardiac arrhythmia. *Heart*. 2011;97:698–708. doi: [10.1136/hrt.2010.209304](https://doi.org/10.1136/hrt.2010.209304)
- Meloux A, Rigal E, Rochette L, Cottin Y, Bejot Y, Vergely C. Ischemic stroke increases heart vulnerability to ischemia-reperfusion and alters myocardial cardioprotective pathways. *Stroke*. 2018;49:2752–2760. doi: [10.1161/STROKEAHA.118.022207](https://doi.org/10.1161/STROKEAHA.118.022207)
- Ishikawa H, Tajiri N, Vasconcellos J, Kaneko Y, Mimura O, Dezawa M, Borlongan CV. Ischemic stroke brain sends indirect cell death signals to the heart. *Stroke*. 2013;44:3175–3182. doi: [10.1161/STROKEAHA.113.001714](https://doi.org/10.1161/STROKEAHA.113.001714)
- Lin H-B, Wei G-S, Li F-X, Guo W-J, Hong P, Weng Y-Q, Zhang Q-Q, Xu S-Y, Liang W-B, You Z-J, et al. Macrophage-NLRP3 inflammasome activation exacerbates cardiac dysfunction after ischemic stroke in a mouse model of diabetes. *Neurosci Bull*. 2020;36:1035–1045. doi: [10.1007/s12264-020-00544-0](https://doi.org/10.1007/s12264-020-00544-0)
- Samuels MA. The brain-heart connection. *Circulation*. 2007;116:77–84. doi: [10.1161/CIRCULATIONAHA.106.678995](https://doi.org/10.1161/CIRCULATIONAHA.106.678995)
- Yan T, Chen Z, Chopp M, Venkat P, Zacharek A, Li W, Shen Y, Wu R, Li L, Landschoot-Ward J, et al. Inflammatory responses mediate brain-heart interaction after ischemic stroke in adult mice. *J Cereb Blood Flow Metab*. 2020;40:1213–1229. doi: [10.1177/0271678X18813317](https://doi.org/10.1177/0271678X18813317)
- Zaman R, Epelman S. Resident cardiac macrophages: heterogeneity and function in health and disease. *Immunity*. 2022;55:1549–1563. doi: [10.1016/j.immuni.2022.08.009](https://doi.org/10.1016/j.immuni.2022.08.009)
- Bajpai G, Bredemeyer A, Li W, Zaitsev K, Koenig AL, Lokshina I, Mohan J, Ivey B, Hsiao H-M, Weinheimer C, et al. Tissue resident CCR2⁻ and CCR2⁺ cardiac macrophages differentially orchestrate monocyte recruitment and fate specification following myocardial injury. *Circ Res*. 2019;124:263–278. doi: [10.1161/CIRCRESAHA.118.314028](https://doi.org/10.1161/CIRCRESAHA.118.314028)
- Revelo X, Parthiban P, Chen C, Barrow F, Fredrickson G, Wang HG, Yücel D, Herman A, van Berlo JH. Cardiac resident macrophages prevent fibrosis and stimulate angiogenesis. *Circ Res*. 2021;129:1086–1101. doi: [10.1161/CIRCRESAHA.121.319737](https://doi.org/10.1161/CIRCRESAHA.121.319737)
- Epelman S, Lavine KJ, Beaudin AE, Sojka DK, Carrero JA, Calderon B, Brija T, Gautier EL, Ivanov S, Satpathy AT, et al. Embryonic and adult-derived resident cardiac macrophages are maintained through distinct mechanisms at steady state and during inflammation. *Immunity*. 2014;40:91–104. doi: [10.1016/j.immuni.2013.11.019](https://doi.org/10.1016/j.immuni.2013.11.019)
- Bajpai G, Schneider C, Wong N, Bredemeyer A, Hulsmans M, Nahrendorf M, Epelman S, Kreiseld L, Liu Y, Itoh A, et al. The human heart contains distinct macrophage subsets with divergent origins and functions. *Nat Med*. 2018;24:1234–1245. doi: [10.1038/s41591-018-0059-x](https://doi.org/10.1038/s41591-018-0059-x)
- Patel B, Bansal SS, Ismahil MA, Hamid T, Rokosh G, Mack M, Prabhu SD. CCR2 monocyte-derived infiltrating macrophages are required for adverse cardiac remodeling during pressure overload. *JACC Basic Transl Sci*. 2018;3:230–244. doi: [10.1016/j.jacbs.2017.12.006](https://doi.org/10.1016/j.jacbs.2017.12.006)
- Prabhu SD, Frangogiannis NG. The biological basis for cardiac repair after myocardial infarction: from inflammation to fibrosis. *Circ Res*. 2016;119:91–112. doi: [10.1161/CIRCRESAHA.116.303577](https://doi.org/10.1161/CIRCRESAHA.116.303577)
- Liao X, Chang E, Tang X, Watanabe I, Zhang R, Jeong H-W, Adams RH, Jain MK. Cardiac macrophages regulate isoproterenol-induced Takotsubo-like cardiomyopathy. *JCI Insight*. 2022;7:e156236. doi: [10.1172/jci.insight.156236](https://doi.org/10.1172/jci.insight.156236)
- Bieber M, Werner RA, Tanai E, Hofmann U, Higuchi T, Schuh K, Heuschmann PU, Frantz S, Ritter O, Kraft P, et al. Stroke-induced chronic systolic dysfunction driven by sympathetic overactivity. *Ann Neurol*. 2017;82:729–743. doi: [10.1002/ana.25073](https://doi.org/10.1002/ana.25073)
- Reyes-Garcia MG, Garcia-Tamayo F. A neurotransmitter system that regulates macrophage pro-inflammatory functions. *J Neuroimmunol*. 2009;216:20–31. doi: [10.1016/j.jneuroim.2009.06.024](https://doi.org/10.1016/j.jneuroim.2009.06.024)
- Fu Y-Y, Peng S-J, Lin H-Y, Pasricha PJ, Tang S-C. 3-D imaging and illustration of mouse intestinal neurovascular complex. *Am J Physiol Gastrointest Liver Physiol*. 2013;304:G1–G11. doi: [10.1152/ajpgi.00209.2012](https://doi.org/10.1152/ajpgi.00209.2012)
- Godinho-Silva C, Cardoso F, Veiga-Fernandes H. Neuro-immune cell units: a new paradigm in physiology. *Annu Rev Immunol*. 2019;37:19–46. doi: [10.1146/annurev-immunol-042718-041812](https://doi.org/10.1146/annurev-immunol-042718-041812)
- Pirzgalska RM, Seixas E, Seidman JS, Link VM, Sánchez NM, Mahú I, Mendes R, Gres V, Kubasova N, Morris I, et al. Sympathetic neuron-associated macrophages contribute to obesity by importing and metabolizing norepinephrine. *Nat Med*. 2017;23:1309–1318. doi: [10.1038/nm.4422](https://doi.org/10.1038/nm.4422)
- Charan J, Kantharia ND. How to calculate sample size in animal studies? *J Pharmacol Pharmacother*. 2013;4:303–306. doi: [10.4103/0976-500X.119726](https://doi.org/10.4103/0976-500X.119726)
- Huang X-X, Zhang Q-Q, Pang X-X, Lin H-B, He W-Y, Yuan D, Guo W-J, Zhang H-F, Li F-X. Role of galectin-3 in cardiac dysfunction induced by subarachnoid hemorrhage. *Exp Neurol*. 2023;365:114418. doi: [10.1016/j.expneurol.2023.114418](https://doi.org/10.1016/j.expneurol.2023.114418)
- Krahn AD, Tfelt-Hansen J, Tadros R, Steinberg C, Semsarian C, Han H-C. Latent causes of sudden cardiac arrest. *JACC Clin Electrophysiol*. 2022;8:806–821. doi: [10.1016/j.jacep.2021.12.014](https://doi.org/10.1016/j.jacep.2021.12.014)
- Chen H-R, Chen C-W, Kuo Y-M, Chen B, Kuan IS, Huang H, Lee J, Anthony N, Kuan C-Y, Sun Y-Y. Monocytes promote acute neuroinflammation and become pathological microglia in neonatal hypoxic-ischemic brain injury. *Theranostics*. 2022;12:512–529. doi: [10.7150/thno.64033](https://doi.org/10.7150/thno.64033)
- Chen Z, Feng X, Herting CJ, Garcia VA, Nie K, Pong WW, Rasmussen R, Dwivedi B, Seby S, Wolf SA, et al. Cellular and molecular identity of tumor-associated macrophages in glioblastoma. *Cancer Res*. 2017;77:2266–2278. doi: [10.1158/0008-5472.CAN-16-2310](https://doi.org/10.1158/0008-5472.CAN-16-2310)
- Scholzen T, Gerdes J. The Ki-67 protein: from the known and the unknown. *J Cell Physiol*. 2000;182:311–322. doi: [10.1002/\(SICI\)1097-4652\(200003\)182:3<311::AID-JCP1>3.0.CO;2-9](https://doi.org/10.1002/(SICI)1097-4652(200003)182:3<311::AID-JCP1>3.0.CO;2-9)
- Zhang H, Yang K, Chen F, Liu Q, Ni J, Cao W, Hua Y, He F, Liu Z, Li L, et al. Role of the CCL2-CCR2 axis in cardiovascular disease: pathogenesis and clinical implications. *Front Immunol*. 2022;13:975367. doi: [10.3389/fimmu.2022.975367](https://doi.org/10.3389/fimmu.2022.975367)
- Raghu H, Lepus CM, Wang Q, Wong HH, Lingampalli N, Oliviero F, Punzi L, Giori NJ, Goodman SB, Chu CR, et al. CCL2/CCR2, but not CCL5/CCR5, mediates monocyte recruitment, inflammation and cartilage destruction in osteoarthritis. *Ann Rheum Dis*. 2017;76:914–922. doi: [10.1136/annrheumdis-2016-210426](https://doi.org/10.1136/annrheumdis-2016-210426)
- Sansonetti M, Waleczek FJG, Jung M, Thum T, Perbellini F. Resident cardiac macrophages: crucial modulators of cardiac (patho)physiology. *Basic Res Cardiol*. 2020;115:77. doi: [10.1007/s00395-020-00836-6](https://doi.org/10.1007/s00395-020-00836-6)
- Mu X, Li Y, Fan G-C. Tissue-resident macrophages in the control of infection and resolution of inflammation. *Shock*. 2021;55:14–23. doi: [10.1097/SHK.0000000000001601](https://doi.org/10.1097/SHK.0000000000001601)
- Zhang J, Liu X, Wan C, Liu Y, Wang Y, Meng C, Zhang Y, Jiang C. NLRP3 inflammasome mediates M1 macrophage polarization and IL-1 β production in inflammatory root resorption. *J Clin Periodontol*. 2020;47:451–460. doi: [10.1111/jcpe.13258](https://doi.org/10.1111/jcpe.13258)
- Gervasi NM, Scott SS, Aschrafi A, Gale J, Vohra SN, MacGibeny MA, Kar AN, Gioio AE, Kaplan BB. The local expression and trafficking of tyrosine hydroxylase mRNA in the axons of sympathetic neurons. *RNA*. 2016;22:883–895. doi: [10.1261/rna.053272.115](https://doi.org/10.1261/rna.053272.115)
- Prendiville TW, Ma Q, Lin Z, Zhou P, Gale A, Pu WT. Ultrasound-guided transthoracic intramyocardial injection in mice. *J Vis Exp*. 2014;e51566. doi: [10.3791/51566-v](https://doi.org/10.3791/51566-v)
- Gao Y-J, Ji R-R. c-Fos and pERK, which is a better marker for neuronal activation and central sensitization after noxious stimulation and tissue injury? *Open Pain J*. 2009;2:11–17. doi: [10.2174/1876386300902010011](https://doi.org/10.2174/1876386300902010011)

36. Sörös P, Hachinski V. Cardiovascular and neurological causes of sudden death after ischaemic stroke. *Lancet Neurol.* 2012;11:179–188. doi: [10.1016/S1474-4422\(11\)70291-5](https://doi.org/10.1016/S1474-4422(11)70291-5)
37. Scheitz JF, Sposato LA, Schulz-Menger J, Nolte CH, Backs J, Endres M. Stroke–heart syndrome: recent advances and challenges. *J Am Heart Assoc.* 2022;11:e026528. doi: [10.1161/JAHA.122.026528](https://doi.org/10.1161/JAHA.122.026528)
38. Scheitz JF, Nolte CH, Doehner W, Hachinski V, Endres M. Stroke–heart syndrome: clinical presentation and underlying mechanisms. *Lancet Neurol.* 2018;17:1109–1120. doi: [10.1016/S1474-4422\(18\)30336-3](https://doi.org/10.1016/S1474-4422(18)30336-3)
39. Ruthirago D, Julayanont P, Tantrachoti P, Kim J, Nugent K. Cardiac arrhythmias and abnormal electrocardiograms after acute stroke. *Am J Med Sci.* 2016;351:112–118. doi: [10.1016/j.amjms.2015.10.020](https://doi.org/10.1016/j.amjms.2015.10.020)
40. Li Y, Fitzgibbons TP, McManus DD, Goddeau RP, Silver B, Henninger N. Left ventricular ejection fraction and clinically defined heart failure to predict 90-day functional outcome after ischemic stroke. *J Stroke Cerebrovasc Dis.* 2019;28:371–380. doi: [10.1016/j.jstrokecerebrovasdis.2018.10.002](https://doi.org/10.1016/j.jstrokecerebrovasdis.2018.10.002)
41. Wong NR, Mohan J, Kopecky BJ, Guo SC, Du LX, Leid J, Feng GS, Lokshina I, Dmytrenko O, Luehmann H, et al. Resident cardiac macrophages mediate adaptive myocardial remodeling. *Immunity.* 2021;54:2072–2088. doi: [10.1016/j.immuni.2021.07.003](https://doi.org/10.1016/j.immuni.2021.07.003)
42. Zhang K, Wang Y, Chen S, Mao J, Jin Y, Ye H, Zhang Y, Liu X, Gong C, Cheng X, et al. TREM2hi resident macrophages protect the septic heart by maintaining cardiomyocyte homeostasis. *Nat Metab.* 2023;5:129–146. doi: [10.1038/s42255-022-00715-5](https://doi.org/10.1038/s42255-022-00715-5)
43. Strowig T, Henao-Mejia J, Elinav E, Flavell R. Inflammasomes in health and disease. *Nature.* 2012;481:278–286. doi: [10.1038/nature10759](https://doi.org/10.1038/nature10759)
44. Lu Y, Huang Y, Li J, Huang J, Zhang L, Feng J, Li J, Xia Q, Zhao Q, Huang L, et al. Eosinophil extracellular traps drive asthma progression through neuro-immune signals. *Nat Cell Biol.* 2021;23:1060–1072. doi: [10.1038/s41556-021-00762-2](https://doi.org/10.1038/s41556-021-00762-2)
45. Klein Wolterink RGJ, Wu GS, Chiu IM, Veiga-Fernandes H. Neuroimmune interactions in peripheral organs. *Annu Rev Neurosci.* 2022;45:339–360. doi: [10.1146/annurev-neuro-111020-105359](https://doi.org/10.1146/annurev-neuro-111020-105359)
46. Pruenster M, Immler R, Roth J, Kuchler T, Bromberger T, Napoli M, Nussbaumer K, Rohwedder I, Wackerbarth LM, Piantoni C, et al. E-selectin-mediated rapid NLRP3 inflammasome activation regulates S100 A8/S100A9 release from neutrophils via transient gasdermin D pore formation. *Nat Immunol.* 2023;24:2021–2031. doi: [10.1038/s41590-023-01656-1](https://doi.org/10.1038/s41590-023-01656-1)